Onset of nonlinear saturation for Rayleigh-Taylor growth in the presence of a full spectrum of modes

Steven W. Haan

Lawrence Livermore National Laboratory, Livermore, California 94550

It is generally recognized that a single Rayleigh-Taylor unstable mode grows exponentially, proportional to the initial amplitude, until the amplitude is about $\frac{1}{10}$ to $\frac{1}{5}$ of the wavelength. The growth then becomes nonlinear, and the mode evolves into spikes and bubbles. This paper considers how this picture of the transition to nonlinearity changes when, instead of there being a single mode, there is a full spectrum of modes. We argue that nonlinear behavior begins whenever the sum of modes over a specified small region of k space becomes comparable to the wavelength. In the case of a single mode, this reduces to the usual comparison of the mode's amplitude with its wavelength λ. But if the modal amplitudes are smooth functions of k, the modes begin to saturate when their amplitude is comparable to λ^2/R times a dimensionless scale factor; here, R is the radius in spherical geometry, or the length of the surface in planar geometry. Given this new notion of the amplitude at which nonlinear saturation begins, we construct a simple model to estimate the net perturbation resulting from a broadband initial spectrum. We assume that modes grow exponentially until saturation occurs, and then the growth of the individual modes becomes linear in time. The model predictions in two and three dimensions are compared with Read and Young's experiments [Atomic Weapons Research Establishment Report No. 011/83, Aldermasten, 1983 (unpublished)], and to Youngs's calculations [Physica **12D**, 32 (1984)]. The experimental results are used to set the single parameter characterizing the onset of nonlinearity. The model provides a complete description of a weak dependence on initial amplitude. The model can be easily extended to any situation for which one can estimate single-mode growths; results are presented regarding effects on multimode growth of spherical geometry, ablation stabilization, and interface coupling.

I. INTRODUCTION

An interface between two fluids is unstable when a lower-density fluid pushes against and accelerates another fluid of higher density. This perturbation growth is known as the Rayleigh-Taylor instability.[1,2] Estimating its effect is important for inertial confinement fusion (ICF) because imploding targets generally have interfaces that are unstable during part of the implosion. These instabilities can reduce the target yield. References 3 and 4 summarize and discuss much of the work in this area. It is generally recognized that a mode with wavelength λ grows exponentially, proportional to its initial amplitude, until it reaches an amplitude of about 0.1λ. Various factors are known to influence the growth during this phase, such as ablative effects, spherical convergence, and interface coupling. The other extreme—very later-time behavior arising from an initial condition with multiple modes—is also becoming better characterized, mostly as a result of the important work of Youngs and co-workers.[5,6] At this time it is not clear how the various other influences just mentioned affect this late-time behavior, which has been characterized mostly for constant acceleration, incompressible fluids, and planar geometry.

In this article, we consider the amplitude at which the growth of a mode begins to be nonlinear, in the presence of a full spectrum of modes. A group of modes with nearly equal wave vectors can combine constructively over a region of the surface, producing a net amplitude much larger than the modes' individual amplitudes. Thus, nonlinear saturation can begin well before the amplitude of the individual modes reaches 0.1λ. In Secs. II and III we consider arguments regarding the amplitude at which the saturation begins in the multimode situation.

The other basic point emphasized in this article is that the net perturbation in the multimode situation must be estimated by summing the modes. Perhaps this is obvious, but there is a tendency among workers in the field (as reviewed in Refs. 3 and 4) to relate the net amplitude to the amplitude of the dominant mode. Using sums over modes, as we do here, can give a quite different understanding of the relationships between modal amplitudes and net perturbation amplitudes.

In Sec. IV we define a simple model based on these considerations. The onset of saturation is determined from the arguments of Sec. III. Then, once a mode reaches saturated amplitude, it is assumed to grow linearly in time. (Actually we will borrow from Crowley,[7] a generalized way to realize this, which can then be used for situations other than constant acceleration.) The net perturbation is determined by summing over all modes. No nonlinear mode coupling is included, except that, as mentioned above, the onset of saturation is influenced by the constructive interference of modes with similar wave vectors. The model allows one to estimate the multimode

perturbation growth for any situation in which one can estimate the single-mode growths and initial amplitudes.

Section V presents the application of the model to various situations of interest. First, we consider constant acceleration in planar geometry. The resulting net bubble amplitude is nearly proportional to gt^2 times the Atwood number, with a weak dependence on initial amplitude. Comparison with the experiments of Read and Youngs allows us to set the single parameter characterizing the model. Then, we consider planar geometry in two dimensions, and the effects on the multimode growth of spherical geometry, ablative stabilization, and interface coupling.

Section VI contains a discussion of the model and its limitations. In summary, the conclusion is that the model gives results close to what one would like to see for the various situations considered. Whether the results are in fact correct will await detailed comparison with experiments or code calculations. It is clear that the model has limitations, both in terms of the physics that has been neglected, and in terms of its practical applicability, and we discuss circumstances for which it is not expected to be useful.

II. BASIC DEFINITIONS

We are concerned with perturbations on an interface between two materials in an imploding ICF capsule. The most commonly considered situation is a Rayleigh-Taylor unstable interface: a fluid of density ρ_L pushes against and accelerates or decelerates another fluid of higher density ρ_H. A perturbation of wavelength λ on the interface is unstable and, for a small amplitude perturbation with constant acceleration, grows exponentially with growth rate

$$\gamma = \sqrt{gk\alpha} \ . \tag{1}$$

Here, k is the wave number $2\pi/\lambda$, g is the acceleration, and α is the Atwood number,

$$\alpha = \frac{\rho_H - \rho_L}{\rho_H + \rho_L} \ . \tag{2}$$

The growth of a single mode of wavelength λ is known to slow down when the amplitude becomes comparable to the wavelength.[3,4] We will say that the growth begins to slow when the amplitude is $\eta\lambda$, where η is in the range 0.05–0.15. Eventually, a single mode evolves into "bubbles" of low-density fluid moving with constant velocity v_B into the high-density fluid, and "spikes" of high-density fluid moving into the low-density fluid. Even for the multimode case, it is common to refer to the penetration of low-density fluid into the high-density fluid as the "bubble amplitude," and of the high-density fluid into the low-density fluid as the "spike amplitude." We will employ the same usage.

For a slightly perturbed spherical system, we can identify the interface at time t with a function $R(\hat{\Omega}, t)$, representing the radius of the interface (from an appropriate defined center) in direction $\hat{\Omega}$. We will often leave the time dependence implicit. R can be expanded in spherical harmonics as

$$R(\hat{\Omega}, t) = \sum_{l,m} R_{lm}(t) Y_{lm}(\hat{\Omega}) \ , \tag{3}$$

where

$$R_{lm} = \int d\hat{\Omega} \, Y_{lm}^*(\hat{\Omega}) R(\hat{\Omega}) \ . \tag{4}$$

The center can be chosen to make the $l = 1$ modes vanish. A useful quantity for estimating the net perturbation is the rms deviation of R from its average R_0:

$$\sigma = \left[\frac{1}{4\pi} \int d\hat{\Omega} [R(\hat{\Omega}) - R_0]^2 \right]^{1/2} \ . \tag{5}$$

This deviation is also determined by the quadrature sum of all the modal amplitudes:

$$\sigma = \left[\frac{1}{4\pi} \sum_{l(>1)} \sum_m |R_{lm}|^2 \right]^{1/2} \ . \tag{6}$$

Similarly, for plane geometry the interface is $z(\mathbf{x}, t)$, where $\mathbf{x}$ is a two-dimensional vector (x, y). The variables x and y range over $(0, L)$. The perturbation is expanded as

$$z(\mathbf{x}, t) = \sum_{\mathbf{k}} z_{\mathbf{k}}(t) e^{i\mathbf{k}\cdot\mathbf{x}} \ , \tag{7}$$

where $\mathbf{k}$ has discrete allowed values $(2\pi n/L, 2\pi m/L)$ for integers n, m. The inverse transform is

$$z_{\mathbf{k}}(t) = \frac{1}{L^2} \int d\mathbf{x} \, e^{-i\mathbf{k}\cdot\mathbf{x}} z(\mathbf{x}, t) \ . \tag{8}$$

The deviation is

$$\sigma = \left[\frac{1}{L^2} \int d\mathbf{x} [z(\mathbf{x}, t) - z_0]^2 \right]^{1/2} \tag{9}$$

$$= \left[\sum_{\mathbf{k}(\neq 0)} |z_{\mathbf{k}}|^2 \right]^{1/2} \ . \tag{10}$$

It is necessary to compare briefly the formalisms for spherical and planar geometries. For ICF applications we are interested in the former, and the applications here will use primarily the spherical harmonic decomposition rather than the Fourier decomposition appropriate to planar geometry. But there are several points at which a connection must be made.

The modes in planar and spherical geometry are best related via the eigenvalue of the two-dimensional part of the Laplacian operator, that is, k^2 in planar geometry and $l(l+1)/R_0^2$ in spherical geometry. The spherical harmonic modes are not simple waves, and so one cannot really define a wavelength for them. Nevertheless, we will use the connection defined by the Laplacian eigenvalues to refer to the "wavelength" of the modes:

$$k^2 = (2\pi/\lambda)^2 = l(l+1)/R_0^2 \ . \tag{11}$$

It is true that for $l \gg 1$ and at positions on the sphere not too near the pole, a given Y_{lm} can be approximately represented as a superposition of planar modes whose wave vectors point in different directions but are of magnitude k. We will not have to utilize the details of this correspondence. Furthermore, since we are concerned

with an approximate analysis depending on $l \gtrsim 10$, we will set $l+1$ to l in Eq. (11).

The relative normalization of the z_k and R_{lm} can be ascertained by writing σ^2 in the same form using the two formalisms. Assuming azimuthal symmetry and taking into account the density of states, we can write Eq. (10) as

$$\sigma^2 = \frac{L^2}{2\pi} \int_0^\infty dk \, k |z_k|^2 . \tag{12}$$

Similarly, we rewrite Eq. (6) (for situations where $l \gg 1$) as an integral over $k = l/R$, giving

$$\sigma^2 = \frac{R^2}{2\pi} \int_0^\infty dk \, k |R_{lm}|^2 . \tag{13}$$

Therefore, if we take $L = R$, the z_k and R_{lm} have the same effective normalization, including the density-of-states factors.

Regarding the time evolution for a given l value, the equivalent of Eq. (1) in spherical geometry is well known for incompressible fluids and is discussed in Ref. 3. However, compressibility effects generally play an important role in ICF implosions, and the applicability of incompressible theory is questionable. Determining the actual growth of individual modes for compressible fluids in spherical geometry is nontrivial. Such calculations will be discussed below as relevant to the model presented here. In general, the linear growth rate for spherical modes depends on the value of l, and not on m, because of spherical symmetry. For l sufficiently large, we expect the solutions in spherical geometry to reduce to the planar limit according to the correspondence given in Eq. (11). This is the case for the exact solution for incompressible fluids.

Another issue is the saturation of growth, beginning at $\eta\lambda$ for a planar mode. For a pure spherical harmonic mode of amplitude R_{lm}, the deviation from sphericity is generally R_{lm} times some fraction less than but of order unity. The rms amplitude is $R_{lm}/\sqrt{4\pi}$. We might accordingly expect that the onset of saturation for a spherical harmonic mode would occur at some amplitude differing from $\eta\lambda$ by a factor of order unity. There are additional complications that could occur in spherical geometry. First, the saturation of a spherical harmonic mode probably does not occur simultaneously over the entire sphere, since the "typical" amplitude depends somewhat on latitude. Also, the saturation probably depends on m, whereas λ (as taken from the eigenvalue of the Laplacian, and which characterizes the linear growth) depends only on l. Fortunately, it is not necessary to analyze these issues in detail for the development carried out below. The required saturation modeling can be normalized directly in a manner independent of these details.

III. ONSET OF NONLINEARITY

Given the notion of utilizing Eqs. (6) or (10) in the nonlinear regime, it is immediately apparent that we must revise the conventional prescription for the amplitude at which the growth of a mode saturates. If all modes were allowed to become comparable to their wavelengths (or to their wavelengths times any constant), the sum defining σ

diverges. A cutoff could enter because the initial amplitudes would eventually fall off with increasing k, but it does not seem reasonable for the late-time net bubble penetration to be determined by a cutoff in initial value. A cutoff could also occur because of ablative stabilization or viscosity. But, in general, it is evident that nonlinear effects are likely to occur at an amplitude smaller than $\eta\lambda$, in the case of interest where there are a large number of modes.

There are various nonlinear effects that could play a role in preventing growth to $\eta\lambda$, but there is also a basic conceptual error one makes in comparing a single-mode amplitude to $\eta\lambda$. The nature of that error is best understood by looking at a specific case. Consider a surface (say, in planar geometry as defined above) that is covered with growing Rayleigh-Taylor ripples of wavelength λ and typical peak-to-peak amplitude of $2\eta\lambda$. This would be generally recognized as marginally saturated. However, there are two ways one could mathematically construct such a perturbed surface. One, of course, is to have a single (real) Fourier mode of wave vector $\mathbf{k}$ and amplitude $\eta\lambda$. The other is to have a sum of modes, of various wave vectors all close to $\mathbf{k}$ and $-\mathbf{k}$, with rms amplitude σ of $\eta\lambda/\sqrt{2}$. Locally the perturbation with nonzero bandwidth would look just like the pure mode. If all modes $\mathbf{k}'$ contributing to the sum have $|\mathbf{k}-\mathbf{k}'| < \epsilon k$ or $|\mathbf{k}+\mathbf{k}'| < \epsilon k$, where ϵ is some fraction less than 1, the finite bandwidth could be distinguished from a pure mode only with measurements extending over a distance large enough to see the phase differences arising from the different elements in the superposition—i.e., over distances of order λ/ϵ. So if ϵ is less than, say, $\frac{1}{2}$, the perturbation with the finite bandwidth should behave qualitatively the same as the pure mode, saturating when its net real amplitude is about $\eta\lambda$. But the amplitude of the individual modes is completely different from $\eta\lambda$. Let $S(k)$ denote the amplitude of these marginally saturated modes. We can write an expression for this amplitude by equating $\eta\lambda$ to $\sqrt{2}$ times the rms amplitude of the perturbation. (The factor $\sqrt{2}$ relates the rms amplitude of the sinusoidal perturbation to the peak amplitude.) The rms sum is given by the product of three factors: the area in k space over which we are summing, the density of states, and the square amplitude of the individual modes. That is,

$$\eta\lambda = \sqrt{2}\{2\pi(\epsilon k)^2[L^2/(2\pi)^2]S^2(k)\}^{1/2} . \tag{14}$$

Solving for $S(k)$ gives

$$S(k) = 2\pi\sqrt{\pi}\eta/(L\epsilon k^2) \tag{15}$$

for the amplitude of the individual modes when the resulting net perturbation is marginally saturated.[8]

Now consider the more general case with a full spectrum of modes. As these modes grow there is the possibility for a wide variety of nonlinear effects. Modes of quite different wavelength can interact via nonlinear processes, which we are not concerned with here. The point we do emphasize is that modes of very similar wave vectors interact in the same way as was considered above in the special case where there was only one band of modes.

Any modes whose wave vectors are close enough that their perturbations can stay in phase for a wavelength or two affect each other's saturation, in that whether or not saturation occurs is determined by their sum rather than by their individual amplitudes. Thus, we must use Eq. (15) in this situation as well, in order to determine the amplitude at which modes are large enough to be nonlinear. In this context, the parameter ϵ defines how close the wave vectors of two modes must be in order for them to interfere constructively over a sufficiently large area to influence each other's saturation. Of course, other nonlinear effects could influence modal growth long before this amplitude is reached, but if the amplitudes get to $S(k)$ they themselves become nonlinear, in exactly the same sense that a single mode becomes nonlinear at $\eta\lambda$.

The argument above was made for planar geometry. In spherical geometry it is more difficult to envision the various interference effects, the definitions of "similar" modes, and so on. So it is not trivial to modify the above arguments to spherical geometry. Nevertheless, simply from the parallels between the two formalisms, it is clear that the spherical analogue to Eq. (15) must be

$$S(l,R_0)=\nu R_0/l^2 \ , \tag{16}$$

where $S(l,R_0)$ is defined to be the saturation level of mode l,m, in the presence of a dense spectrum of modes, at average radius R_0. Using the planar to spherical equivalence represented by Eqs. (12) and (13), we can determine that the quantity ν is approximately given by

$$\nu \cong 2\pi^{3/2}\eta/\epsilon \ . \tag{17}$$

Note that ϵ and η have combined multiplicatively, leaving only the one parameter ν. If η is given a traditional value of $1/(2\pi)$, and ϵ is $\frac{1}{4}$ (so that the saturation of a mode is influenced by modes whose wavelengths are similar enough that they can stay in phase for somewhat more than one wavelength), then ν is 7. We will normalize ν below directly to the experiments of Read and Youngs; from first principles we might expect it to be in the range 1–10.

Our confidence in this result is enhanced considerably by examining how the saturation modeling in spherical geometry should scale with radius. In fact, the functional form for $S(l,R_0)$ is determined within a multiplicative constant by two scaling principles. The first scaling principle is that the amplitude at which saturation sets in, for a given l, should be proportional to the overall radius. The wavelength is proportional to radius, and this is the sort of scaling one sees if all amplitudes are scaled with radius to give various similar configurations, with the only difference being the overall scale. It is intuitively obvious that the saturation should share this overall scaling. This scaling principle can be written as

$$S(l,R_0)=R_0 s_1(l) \ , \tag{18}$$

where $s_1(l)$ is an unspecified function of l alone.

For the second scaling rule, we consider what happens at large R_0 if the rms perturbation amplitude is fixed. We will argue that in this case the amplitude of any one of the contributing modes should scale as $1/R_0$ (except

for the special case of a pure mode). Consider a sphere of radius R_0 on which there are ripples of typical wavelength λ and amplitude a_0 (where λ and a_0 are fixed as we consider various sphere radii). We are concerned with the situation where R_0 is much larger than λ and a_0. If these ripples originate from a pure mode, the spherical harmonic amplitude of this mode is a_0 times a factor of order unity and is independent of R_0. But for this pure mode, the phase of the ripples is exactly specified over the entire sphere. In general, we would expect there to be some smaller area over which the phase of the ripples is correlated, which does not scale with R_0. (Equivalently, we could hypothesize an uncertainty in the wavelength.) Assume that the phase is correlated over area $N\lambda^2$, i.e., over solid angle

$$\Delta\Omega=N\lambda^2/(4\pi R_0^2) \ . \tag{19}$$

Now consider the integral defining R_{lm}, Eq. (4), for values of l and m that correspond approximately to the characteristics of the ripples of interest. This integral can be thought of as a sum of random terms, each one representing the integral over a patch of area $N\lambda^2$. In each such area the ripples have a particular phase relationship with Y_{lm}, and the integral over that area is $a_0\Delta\Omega$ times a random phase factor. The total integral, then, is a sum of $4\pi/\Delta\Omega$ random terms, each of order $a_0\Delta\Omega$. So

$$|R_{lm}|\approx a_0\Delta\Omega\sqrt{4\pi/\Delta\Omega} \ . \tag{20}$$

If the correlation area $N\lambda^2$ is fixed as R_0 varies (or if the uncertainty in wavelength is fixed as R_0 varies), then $\Delta\Omega$ is proportional to $1/R_0^2$ and R_{lm} as given by Eq. (20) is proportional to $1/R_0$. There are various other ways one can understand this result: it is related to the fact, evident in Eq. (13), that the "density of states" at given k is proportional to R_0. That is, if one wants the rms amplitude to be independent of R_0, the individual modes must scale with $1/R_0$. Planar Fourier modes scale similarly as one varies the size of the area, as is evident in Eq. (12).

Thus these ripples are represented by a sum of modes whose individual amplitudes scale like $1/R_0$. If the ripples represent just-saturated growth, the individual modes that are combining to form the ripples accordingly experience this saturation at an amplitude proportional to $1/R_0$. Thus the onset of saturation $S(l,R_0)$ must have the scaling property

$$S(l,R_0)=s_2(k)/R_0 \ , \tag{21}$$

where s_2 is some unspecified function of $k=l/R_0$.

These two scaling rules could merely represent the behavior of $S(l,R_0)$ in the appropriate limits. If we assume that they hold exactly, they uniquely determine the functional form of $S(l,R_0)$. That is, Eqs. (18) and (21) require that the amplitude at which saturation begins in the presence of a full spectrum of modes is of the form given by Eq. (16).

This completes our estimate of the amplitude at which saturation occurs. The remainder of this article is concerned with a simple model based on this result.

IV. MODEL BASED ON EXTENSION
OF LINEAR ANALYSIS

The objective here is to formulate a procedure that can be used to estimate the net perturbation amplitude for multimode Rayleigh-Taylor growth. First, we will discuss the linear analysis. Then, we will apply the above result to determine when nonlinearity begins and present a model that seems to us to be the simplest plausible extension into the nonlinear regime.

It is common in Rayleigh-Taylor analysis to estimate net perturbation amplitude by examining the amplitude of the largest mode. As we have already discussed, that can be misleading. Instead, one must use sums of modes.

The quantity we will calculate is the bubble amplitude, which we will denote as B. If the perturbed interface $R(\widehat{\Omega})$ has variations about its mean with peak-to-peak magnitude approximately $2B$, then $[R(\widehat{\Omega})-R_0]^2$ will vary between zero and about B^2. The mean σ^2 of $[R(\widehat{\Omega})-R_0]^2$ will be approximately the mid-range of these variations, i.e., about one-half of B^2. So we will define the bubble amplitude to be $\sqrt{2}\sigma$, where σ is given by Eqs. (5), (6), (9), or (10) as appropriate. This is exact for single-mode sinusoidal perturbations.

In order to calculate the net perturbation in the linear regime, one would determine the initial amplitudes of all modes, determine how they grow (independently, and linearly with their initial amplitudes) to the time of interest, and then use the sum defining σ to determine the net bubble amplitude. If there are multiple seeds, these are presumably randomly phased so that their final amplitudes could be added in quadrature. One necessary condition for applicability of the linear analysis is that all modes be smaller than $S(l,R_0)$ determined above. There is, of course, also the possibility of nonlinear effects, other than simple saturation, that could affect the evolution even before any modes reach $S(l,R_0)$. We will ignore the possibility of these other nonlinear effects.

Now, if some modes have grown past $S(l,R_0)$, how do we estimate the growth? It is generally recognized that single modes, upon reaching saturation, switch from exponential growth to constant velocity bubbles. If the saturation parameter η is chosen appropriately, this transition can be done instantaneously, i.e., the mode amplitude and velocity are continuous across the transfer, and η is chosen so that the velocity at and after the transfer is equal to the known bubble velocity. This approach, attributed to Fermi in Ref. 9, gives results that differ from the best available calculations and measurements by a small factor. We will adopt it for our model, with the generalization that the switch from exponential to linear growth occurs in the multimode environment at $S(l,R_0)$ rather than at $\eta\lambda$. If we knew ϵ and were attempting a first-principles calculation of the net perturbation, the error made in Fermi's approximation might be unacceptable. However, we will normalize v directly to experiment and, therefore, this error will to some degree be normalized out.

A further generalization allows us to easily extend the model to situations where the small-amplitude growth is not necessarily exponential. A way to do this for a fully

general situation was suggested by Crowley.[7] One defines an "unsaturated amplitude" $R_{lm}^u(t)$ as being the amplitude a mode would have grown to if saturation were not an issue. By assumption, this is proportional to the initial amplitude. If $R_{lm}^u(t)$ is greater than the saturation onset function $S(l,R_0)$, then the amplitude is taken to be

$$R_{lm}(t)=S(l,R_0)\left[1+\ln\frac{R_{lm}^u(t)}{S(l,R_0)}\right] . \qquad (22)$$

This logarithmic construction gives growth linear in time for constant acceleration, with the same velocity the mode had when it saturated at amplitude S. In general, the construction gives

$$\frac{d}{dt}R_{lm}=S\gamma(t) , \qquad (23)$$

where

$$\gamma=\frac{1}{R_{lm}^u}\frac{dR_{lm}^u}{dt} \qquad (24)$$

is the growth rate the mode would experience if there were no saturation.

One could argue that the small bubbles should not rise with constant velocity when mix has produced a density gradient that reduces the buoyant force. Another effect generally believed to be important is coupling of short-wavelength modes to seed long-wavelength modes. We are neglecting both these effects, as will be discussed below.

In the nonlinear regime the growth on the spike side becomes different from that on the bubble side. The constant-velocity growth of the R_{lm} quantities is intended to represent the bubble side, so that the reconstructed surface $R(\widehat{\Omega})$ would only be correct on the bubble side of the mean R_0.

In fact, for a large, fully nonlinear perturbation, the interface is not a unique surface, and there are various ways we could define $R(\widehat{\Omega})$. Our objective is to estimate the size of the net perturbation, and we do not need to be specific about how $R(\widehat{\Omega})$ is defined in this case. We will calculate the modal amplitudes R_{lm} as a function of time, and, for such a highly nonlinearly situation, normalize the modeling of the late time $R_{lm}(t)$ so that $\sqrt{2}\sigma$ can still be taken to the bubble amplitude.

Give a value of v, which will be determined below by comparison to Youngs' value of $0.07\alpha gt^2$, the model for bubble growth is now completely defined. A detailed procedure for application to a general case will be laid out just below, after we first consider the spike amplitude. This is known to be somewhat larger than the bubble amplitude, both for single modes and for the multimode case, and is slightly dependent on the value of the Atwood number.[3,5,6] It is possible that this model could be extended to the spikes by using single-mode, late-time spike amplitudes such as those suggested by Crowley.[7] However, ultimately it would be necessary to compare the result with the phenomenological results of Youngs, and it seems more straightforward simply to use the phenomenology. Accordingly, we will assume that the spike

amplitude is proportional to the bubble amplitude, with a proportionality constant that depends on the density ratio per Youngs's results.

The procedure to calculate the bubble and spike amplitudes in general for a spherical implosion is the following.

(i) Estimate the perturbation seeds, as a function of l and m, for all nonuniformities in surface finish, opacity, illumination, and whatever else may be relevant. Of course, one only needs an estimate of the mean value of $|R_{lm}(0)|$ as a smooth function of l and m. The precision with which the initial value must be known can be found by iterating the model as discussed below.

(ii) Using linear analytical modeling or a two-dimensional hydrodynamics code, estimate all the modal amplitudes at the time of interest (not including saturation effects—the amplitudes at this point are strictly proportional to the initial amplitudes, and code calculations should be run with initial amplitudes small enough to guarantee this). If there are multiple seeds, their amplitudes are added in quadrature before considering the saturation modeling. This quadrature sum is the unsaturated amplitude R_{lm}^u discussed above.

(iii) If a mode amplitude is greater than $\nu R/l^2$, it is replaced with the "saturated" amplitude given by Eq. (22). Strictly speaking, this formula is to be used only in the case where there is a large number of modes present, with random phases, and whose mean amplitudes are smooth functions of l and m. If there are pure modes—i.e., modes with amplitudes much larger than those of their neighbors—or if other phase correlations are present, the saturation must be specified by comparing $\eta\lambda$ to a sum of modes with similar wave vectors, in the spirit of the argument above. We will consider this situation further in Sec. V.

(iv) The bubble amplitude is taken to be $\sqrt{2}\sigma$ with σ given by Eq. (6).

(v) The spike amplitude is taken to be $\sqrt{2}\sigma(1+\alpha)$, where α is the Atwood number. This is simply a rough fit to Youngs's results for the spike to bubble ratio.[5] The fit is very approximate but is adequate for our present purposes.

(vi) This procedure can be carried out at various times of interest during the target implosion. Then, given the spike and bubble amplitudes as a function of time, we can attempt to estimate the effect on the observables of interest. This will be nontrivial if amplitudes are significant.

Typically, steps (i)–(iv) are iterated. Upon doing the sum to determine σ in step (iv), we can see which modes and sources are important contributors to the final net amplitude. We then recheck whether these important modes and/or sources have been calculated with sufficient accuracy, and if not we repeat the procedure. As we shall see, how accurately a given mode or source must be calculated varies from problem to problem. In some cases a factor of 2 is significant, while in other cases, where the contributing modes are more heavily saturated or are combined with a large number of other contributing modes and/or sources, changes by orders of magnitude can make little difference in the final net amplitude. It is clear that in some cases this iteration can be

a fairly cumbersome procedure, and in the concluding discussion we will cite this as a principal disadvantage of the model. It is also quite possible that we will be unable to obtain the relevant information regarding single-mode initial amplitudes and growth factors. This completes the description of the procedure. In Sec. V we will apply it to several situations of interest.

V. APPLICATIONS OF THE MODEL FOR ESTIMATING NET PERTURBATIONS

A. Constant acceleration in planar geometry

Obviously, the first thing to check is the experiment of Read and Youngs.[6] In fact, the usual interpretation of this experiment—that short wavelengths in their nonlinear growth seed, via bubble coalescence, the long wavelength modes—stands in fairly clear contradiction to the model we are considering. But while the model disagrees with this interpretation, we will see that it does not disagree with the actual experimental result. (This is not to say that the bubble coalescence phenomenon is never important; a detailed discussion of this issue is presented in Sec. VI, where we review the results of our model.)

In the experiments of interest no initial condition was explicitly set, so we will consider initial values spanning several decades. A lower estimate of the initial value is the perturbation arising from thermal fluctuations. Thermal fluctuations have been observed in light scattering experiments used to measure surface properties, and in our notation have mean-square amplitudes[10]

$$\langle |z_k|^2 \rangle = \frac{1}{L^2} \frac{k_B T}{g\rho + \gamma_s k^2} , \qquad (25)$$

where γ_s is the surface tension, g is the acceleration of gravity (in the stable direction before the experiment, in this equation only), k_B is the Boltzmann constant, and T is the temperature. This expression can be obtained by equating the potential energy in the mode at peak amplitude to $k_B T$. For γ_s we take the value for water of[10] 72 dyn/cm.

Note that, if we were to calculate σ for these modes, the sum over k would diverge logarithmically. In fact, the sum is cut off at large k by quantum effects. Such large-k values have no effect on any calculations we will do at nonzero time.

Given the initial spectrum, the only other independent parameter is $\alpha g t^2$, where g is now the unstable rocket acceleration and α is the Atwood number. The spectrum at any given time is determined by taking the initial amplitude, multiplying each mode by $e^{\gamma t}$, with γ from Eq. (1), and then implementing the saturation modeling described in Sec. IV. (Purists might argue, here and in the following examples, that we should use the hyperbolic cosine rather than the exponential. This is equivalent to a factor of 2 in initial amplitude, which is inconsequential to the applications considered here. Also, we are neglecting the effect of surface tension on the single-mode growth rate.) The spectrum calculated by this prescription for various

times is shown in Fig. 1, where we have used the nominal initial spectrum given by Eq. (25) and set the saturation parameter v to 4 (this choice will be discussed in the following paragraph). Note that the dominant wave vector decreases with time, and that the spectrum is only weakly dependent on the initial spectrum. The bubble amplitude is easily obtained numerically by integrating over k. (The bubble amplitude could also probably be obtained analytically. We will do an example of an analytical calculation in Sec. V B.) The net amplitude is plotted versus agt^2 in Fig. 2. It is quite linear in time and only very weakly dependent on initial amplitude.

Recall that the saturation parameter v was estimated from our basic argument to be in the range of 1–10. The bubble amplitude predicted by the model is almost linear in v. This can be seen numerically in this example by simply varying the parameter; a more detailed description of the dependence on v for a similar situation is worked out analytically in Sec. V B. At any rate, given that the bubble amplitudes plotted in Fig. 2 are nearly linear with v, it is evident that v should be in the range of 3–5 in order to fit the experiments of Read and Youngs. We will take $v=4$ as defining our nominal model.

Read and Youngs also considered situations where they imposed a nonzero initial value on an individual mode. In our model, the saturation of a mode is determined by comparing the sum over a band of modes surrounding it with $\eta\lambda$. If an individual mode is present with amplitude much larger than that of its neighbors, it will dominate this sum. Thus the saturation of this band will be determined by the individual mode: it will grow until it is itself of amplitude $\eta\lambda$ and then saturate, while the growth of the other modes in the band will be suppressed. The nature of this suppression can be clarified somewhat by considering what the surface should look like after the relevant wavelengths have
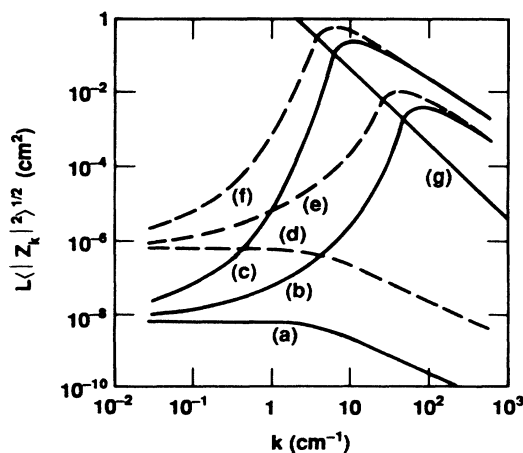
evolved far into the saturated regime. With respect to local measurements on the perturbed surface, the situation with the saturated pure mode will look the same as that with saturated growth of a broader spectrum. But the phase of the saturated ripples will be correlated over the entire surface in the case initiated by the pure mode; in contrast, growth from a broad spectrum would have about the same net amplitude but would lack these long-range phase correlations. The net physical effect will be close to that noted by Read and Youngs: the single mode will grow in approximate correspondence to the usual description, with simultaneous growth of the broadband spectrum whose net perturbation is about $0.07agt^2$. This is the scenario sometimes loosely described as implying that imposed perturbations influence the growth only if their initial amplitude is greater than about $\lambda/100$.

B. Formalism for deceleration in spherical geometry

In the first example, the model was implemented numerically. It is also possible in some situations to do most of the implementation analytically. This can reveal scaling principles that may not be evident from numerical applications. Here we will present an example of a more analytical application.

Consider a perturbed spherical interface, the interior of which is filled with low-density fluid and outside of which is another fluid at higher density. We will take the time of peak velocity as $t=0$, at which time the interface is moving inward with velocity v. The interface subsequently decelerates at constant rate g for a time t in the Rayleigh-Taylor unstable direction. (We will use $v>0$, even though the velocity is inward.) The single-mode growths could be calculated for a given specific situation by various codes and will depend on the details of the trajectory, the convergence, the compressibility, and so on.

FIG. 1. Perturbation spectra for constant acceleration in planar geometry. Curves (a), (b), and (c) are spectra at $agt^2=0$, 5, and 50 cm for a room-temperature initial spectrum. Curves (d), (e), and (f) (dashed lines) are spectra at the same three times as (a), (b), and (c) but with an initial spectrum 100 times as large. Curve (g) is the saturation level $4/k^2$.
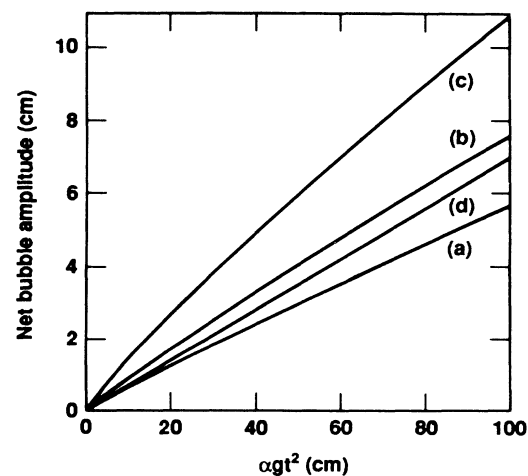
FIG. 2. Calculated bubble amplitude vs agt^2 for constant acceleration in planar geometry. The initial spectrum is room-temperature thermal (a), thermal $\times 100$ (b), or thermal $\times 10^4$ (c). Curve (d) is $0.07agt^2$. The maximum agt^2 is comparable to that in the experiments in Ref. 6. The model parameter v was set to 4 to fit the experimental results.

Our objective is to get an idea of how things scale and not to do a detailed calculation for a specific capsule. Therefore we will use the approximate formula recently cited by Hattori et al.:[11] the growth factor for mode l is given by

$$R_{lm}^u(t)/R_{lm}(0)$$
$$= f_1(t)\exp\left[\int_0^t dt'[\alpha g l/R_0(t')]^{1/2}\right] . \quad (26)$$

We have replaced $[l(l+1)]^{1/2}$ from Ref. 11 with l, and

$$f_1(t) = f(t) = R_0(t)/R_0(0) . \quad (27)$$

The factor $f_1(t)$ in Eq. (26) is slightly unusual, and below we will examine its effect on the predicted net perturbation. Other factors of $R_0(t)/R_0(0)$ will arise in the analysis below. These factors will be written as $f(t)$ and will be kept separate from the factor $f_1(t)$ that originates explicitly in Eq. (26). Later, we can examine the consequences of setting f_1 to 1. Note that the growth described here clearly reduces to the growth described by Eq. (1) if R_0 is much greater than all other length scales at all times.

The other basic ingredient we need is the set of initial amplitudes of the modes. For simplicity, we will assume that the initial amplitudes are independent of l and m, up to a cutoff $l_{\max}$ corresponding to a minimum wavelength $\lambda_{\min}$. The significance of this choice will be considered below. The initial phase of the modes does not enter the formalism directly, although the modeling implicitly assumes random phases. The initial rms surface perturbation $\sigma(0)$ is then related to $R_{lm}(0)$ by Eq. (6) above, which for this case, with $l_{\max} \gg 1$, becomes

$$\sigma(0) = |R_{lm}(0)|l_{\max}/\sqrt{4\pi} . \quad (28)$$

We will see that the initial value will enter our results primarily in the form of a length scale

$$d = \sqrt{\lambda_{\min}\sigma(0)/\nu} = \pi^{1/4}\sqrt{R_0(0)R_{lm}(0)/\nu} . \quad (29)$$

If α and g are constant in time, $R_0(t)$ is quadratic in time and the integral in Eq. (26) is standard.[12] The form of the result depends on the direction of g; here we are assuming $\ddot{R} > 0$. It is convenient to change the mode index from l to $k = l/R_0(0)$. Note that this is the initial wave number and is not time dependent. We will also use $k_{\max} = l_{\max}/R_0(0)$. Evaluating the integral and making these changes, we can write the modal amplitudes as

$$|u(k,t)| = \left[\frac{\sqrt{4\pi}\sigma(0)}{k_{\max}R_0(0)}\right]f_1(t)e^{\sqrt{kD(t)}} , \quad (30)$$

where $u(k,t)$ is the unsaturated amplitude $R_{lm}^u(t)$, and $D(t)$, which is independent of k, is given by

$$D(t) = 2\alpha R_0(0)\left[\ln\frac{\sqrt{2gR_0(t)}+gt-v}{\sqrt{2gR_0(0)}-v}\right]^2 . \quad (31)$$

In the limit of large R_0, D approaches αgt^2. We will see that D is a useful length scale in general.

Now consider the nonlinear saturation. Let $k_s(t)$ be

$l/R_0(0)$ for the mode which is marginally saturated at time t, that is, the mode whose amplitude is just equal to $S[l,R_0(t)]$. The saturation-onset function is, in the formalism being used here,

$$S(k) = vR_0(t)/[kR_0(0)]^2 . \quad (32)$$

To find k_s we equate this function to u as given by Eq. (30), and with some algebra we can write

$$D^2k_s^2e^{\sqrt{Dk_s}} = \sqrt{\pi}(D/d)^2f(t)/f_1(t) . \quad (33)$$

Since D, d, and $f(t)$ are all known, this defines $k_s(t)$ as the solution to this transcendental equation. Both sides have been multiplied by D^2 to show that Dk_s is determined by D/d and $f(t)$. [If k_s, as determined by Eq. (33), is greater than $k_{\max}$, then no modes are saturated. The formalism below can be used for this case by setting all occurrences of k_s to $k_{\max}$. This eliminates the second term in Eqs. (34) and (35).] We can find k_s numerically from Eq. (33) for any particular situation; the predicted bubble penetration is proportional to σ, which is determined by modeling the saturation according to Eq. (22), and then summing per Eq. (6),

$$4\pi\sigma^2(t) = 2R_0^2(0)\int_0^{k_s} dk\, k|u(k,t)|^2$$
$$+ 2R_0^2(0)\int_{k_s}^{k_{\max}} dk\, kS^2(k)\left[1+\ln\frac{|u(k,t)|}{S(k)}\right]^2 . \quad (34)$$

Here we have replaced sums over l by integrals over k. This is correct only if all the significantly contributing modes have $l \gg 1$. The first term in Eq. (34) represents unsaturated modes, and the second the saturated modes. The modal amplitudes $u(k,t)$ are given by Eq. (30). The integrals found by expanding Eq. (34) are standard,[12] and σ^2 can be written as

$$\sigma^2(t) = D^2v^2(d/D)^4\frac{f_1^2F(2\sqrt{Dk_s})}{16\pi^2} + D^2v^2f^2I/2\pi . \quad (35)$$

Here,

$$F(x) = e^x(x^3 - 3x^2 + 6x - 6) + 6 , \quad (36)$$

and

$$I = [(Dk)^{-2}(\beta^2+1)/2 + (Dk)^{-3/2}(4\beta/3 + \tfrac{16}{9}) + (Dk)^{-1}$$
$$+ (Dk)^{-2}(\ln Dk)2\beta + (Dk)^{-3/2}(\ln Dk)(\tfrac{8}{3})$$
$$+ (Dk)^{-2}(\ln Dk)^2]|_{k_{\max}}^{k_s} , \quad (37)$$

where

$$\beta = 2 + \ln\frac{f_1d^2}{f\sqrt{\pi}D^2} . \quad (38)$$

These expressions can now be used to obtain the net perturbation $\sigma(t)$ for any set of parameters specifying an outgoing acceleration.

If we reduce the generality of these expressions slightly, we can get σ into a particularly revealing form. To

STEVEN W. HAAN

get this form we need to use $f_1 = f$ [i.e., leave $f_1 \neq 1$ in Eq. (26)] and take $k_{max} \rightarrow \infty$. Addressing the validity of setting $f_1 = f$ beyond the scope of the present paper. Assuming $k_{max} \rightarrow \infty$ is reasonable for most situations. Except for very small initial amplitudes or very small times, a cutoff is imposed by the saturation modeling and the value obtained for I with finite k_{max} is very close to the ∞ limit. Given these assumptions, the right-hand side of Eq. (35) takes the form of $D^2 v^2 f^2$ times functions of D/d and Dk_s. The latter is in turn a function only of D/d according to Eq. (33) with f_1 set to f. Thus Eq. (35) takes the form

$$\sigma(t) = vD(t)f(t)G(D/d) . \tag{39}$$

Recall that $D(t)$ is $\alpha g t^2$ in the planar limit. Thus σ is nearly proportional to the saturation parameter v, to $f = R_0(t)/R_0(0)$, and to $D \sim \alpha g t^2$. The proportionality "constant" G is a universal transcendental function of the ratio of the two scale lengths D and d (recall that the latter represents the initial condition, as well as depending on v). G is defined conceptually, for given D/d, by solving Eq. (33) for $k_s D$ and substituting the result into the above formulas for F and I (with $k_{max} = \infty$). It is easy to plot G by expressing D/d and G as functions of $k_s D$ and then plotting G versus D/d while varying $k_s D$. G is plotted in Fig. 3. If the bubble amplitude, as predicted by the model, was independent of initial amplitude at late time, G would be a constant at large D/d. This is not the case, at least for meaningful values of D/d. On the other hand, the dependence of G on D/d is extremely weak. Note that the ordinate in Fig. 3 has been normalized so that the quantity plotted would be constant at 0.07 if the bubble amplitude were simply $0.07\alpha g t^2$.

Figure 3 can be used to estimate quickly how the dependence on initial amplitude scales in different situa-
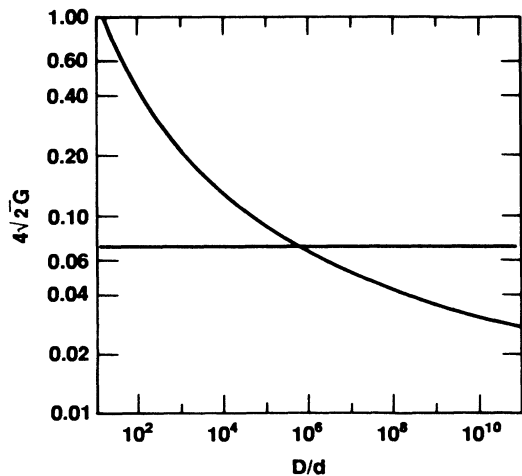
FIG. 3. Bubble amplitude, divided by D, vs D (which is $\alpha g t^2$ in planar geometry) for a "white" initial spectrum. The quantity d defining the abscissa is proportional to the square root of the initial amplitude. The flat line represents bubble amplitude $0.07\alpha g t^2$.

tions. For the Read and Youngs experiments, D is of the order 10 cm and d is of order 10^{-5} cm, so D/d is about 10^6. We have normalized the model, as discussed above, so that $4\sqrt{2}\,G$ is about 0.07 at this point. A decade of change in either direction changes G by about 25%. [Note that a decade of change in d corresponds to two decades in $\sigma(0)$ since d is proportional to $\sigma(0)^{1/2}$.] On the other hand, an ICF capsule might have a D of a few microns, so D/d could be of order 10 to 1000. In that case, the bubble amplitude is a much larger fraction of $\alpha g t^2$, and is much more sensitive to the initial amplitude.

If we consider spectra that are not flat, the form expressed in Eq. (39) is approximately obtained under many, but not all, circumstances. The integral giving σ is usually determined by a band of wavelengths, about a decade wide just above k_s. The integrand in that range is determined by the initial amplitude $u(k,0)$ in that decade, as if d were

$$d_{eff}(l) = \pi^{1/4}[R_0(0)u(l,0)/v]^{1/2} . \tag{40}$$

Since $\sigma(t)$ in Eq. (39) is only weakly dependent on d, the dependence on the initial spectrum is similarly weak. Of course, if this effective d changes by many decades in the course of time, and especially if D/d is smaller than about 10^4, the effective $G(D/d)$ could change by a factor of a few as different portions of the spectrum determine d_{eff}. Note that in many cases the initial spectrum would be a decreasing function of l. In such cases, as time increases, the initial amplitude d_{eff} in the band determining σ increases so that D/d may be less time dependent than in the case of a flat initial spectrum. Then σ would be closer to a constant times $\alpha g t^2$.

It is straightforward to take the large-R_0 limit (i.e., planar geometry) of the above formalism. The only limit that cannot be done by inspection is D, which becomes

$$D = \alpha g t^2 + O(R_0^{-1/2}) . \tag{41}$$

Equations (33) and (35)–(38) can be obtained in the large-R_0 limit by taking $f = f_1 = 1$. None of the other terms in these equations approaches simple limits for planar geometry in general. Note that $\sigma(0)$, d, k_{max}, and k_s are all finite. These quantities retain the same interpretation as they had for finite R_0. Several related quantities, such as $S(k)$ and l_{max}, scale with powers of R_0 in the limit of large R_0. The length scale d is about 10^{-5} cm for the initial thermal noise spectrum considered above.

C. Effect of spherical geometry

Now we will utilize the formalism from Sec. V B in the extreme where the radius is comparable to the net perturbation. We will consider the final perturbation at minimum radius for a target of dimensions taken from Ref. 4, i.e., a shell initially at an inner radius of 150 μm. The inner interface is at peak velocity at a time which we call $t = 0$. This interface then decelerates, at a rate which we will assume to be constant. It finally reaches a minimum radius $R_0(t_{min})$, for which we will consider various values of order 10 μm. To use the above formalism to calculate the perturbation at minimum radius, we

do not need to specify values for all the parameters (i.e., for v, g, etc.). We do need to specify gt^2, $R_0(t_{min})$, v, α, the initial value d (actually representing the surface at peak velocity), and λ_{min} (although the dependence on λ_{min} for a given d is very weak). Of particular interest are the consequences of having the radius comparable to gt^2, so we consider a family of situations that would be identical in the planar limit—that is, we vary $R_0(t_{min})$ while keeping gt^2 fixed. This implies that the radius at peak velocity is $R_0(t_{min}) + gt^2/2$. We will take $gt^2/2 = 30 \ \mu m$, $v = 4$, $\alpha = 0.5$, $\lambda_{min} = 0.01 \ \mu m$ (at peak velocity), and consider various values for d.

Figure 4 shows the calculated bubble penetration as a function of $R_0(t_{min})$. Note that for large R_0 the bubble penetration approaches the planar limit, but as $R_0(t_{min})$ decreases the penetration also decreases. This scaling of the bubble amplitude in spherical geometry is a new prediction of the model. It could, in principal, be checked with multimode numerical simulations similar to those done by Youngs[5] in planar geometry, although these would be constrained to the two-dimensional case discussed in Sec. V E. Figure 4 also shows a curve in which the term f_1 in Eq. (26) has been set to unity. Evidently, this is a much less important effect than the scaling of the saturation modeling with $R_0(t_{min})$. Note that, for a given value of $R_0(t_{min})$, including the f_1 factor has the same effect as reducing the initial value by f_1 (i.e., as reducing d by $\sqrt{f_1}$).
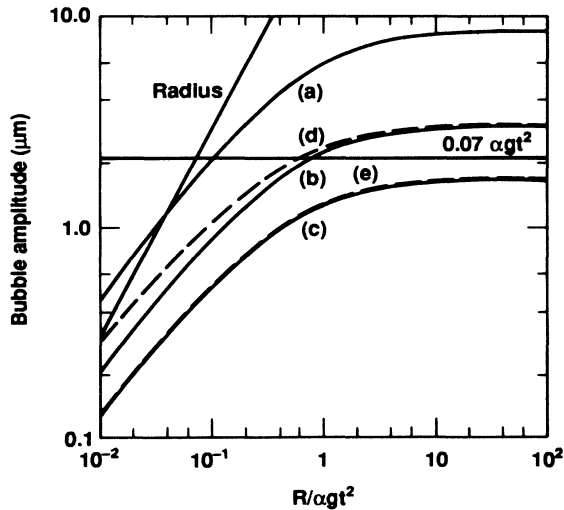
FIG. 4. Calculated bubble amplitude, showing the effect of spherical geometry with final radius R. All curves have $0.5gt^2 = 30 \ \mu m$ and $\alpha = 0.5$, with other parameters as described in the text. Curves (a), (b), and (c) represent growth from white initial spectra characterized by $d = 10^{-1}$, 10^{-3}, and $10^{-5} \ \mu m$, respectively. Dotted line (d) is the same as (b), except that the term f_1 from Eq. (26) has been set to unity. Dotted line (e) is the same as (c), except that λ_{min} has been changed from $10^{-2} \ \mu m$ to $10^{-6} \ \mu m$, at fixed d of $10^{-5} \ \mu m$.

D. A full target implosion with ablation stabilization

Now we consider both the inside and the outside of a single-shell target, and we examine the combined effects of instabilities on both surfaces, along with convergence, ablative stabilization, and interface coupling.

The target dimensions are taken from Ref. 4. The shell is 10 μm thick, initially at an inner radius of 150 μm. We will use a very simple schematic for the dynamics of the implosion. Assume that the ablation surface defining the outside of the shell is accelerated at a constant rate g_1 for time t_1 to a peak velocity of 10^7 cm/s at radius 35 μm. Take the (unperturbed) shell thickness at peak velocity to be 5 μm. The inner surface is subsequently decelerated from 10^7 cm/s at rate g_2 for a time t_2 as it moves from 30 μm to a minimum radius of 10 μm. These parameters are chosen arbitrarily to illustrate the model. For a detailed application to a real target one would use features from a code simulation. Similarly, one would want to use code calculations of single-mode growths as much as possible, rather than the simple analytical formulas used below. The parameters given determine that $t_1 = 2.5$ ns, $g_1 = 4.0 \times 10^{15}$ cm/s^2, $t_2 = 0.4$ ns, and $g_2 = 2.5 \times 10^{16}$ cm/s^2. The Atwood number for the deceleration is assumed to be 0.5.

For an initial condition, suppose for this example that $|R_{lm}(0)|$ is proportional to l^{-1} up to l_{max}. We will consider various values of σ, but we will fix λ_{min} at 1.0×10^{-5} cm (i.e., $l_{max} = 9425$). Of course, $t = 0$ now corresponds to the beginning of the implosion rather than to the peak velocity as in the earlier example. We assume that the initial values are the same on both sides of the shell (in modulus, not necessarily in phase).

First, we consider the ablation front. If the growth rate were classical, i.e., $\sqrt{gk}$, we might expect bubble penetration of order $0.07 \ gt^2$, i.e., 0.14 times the distance moved. These bubbles would penetrate the shell. How might ablation stabilization change this?

The ablation front is stabilized by convection of the perturbed material out through the interface. There does not appear to be a widespread consensus regarding a quantitative description of this effect. Our purpose is to illustrate how the effect can be included in our multimode model, and to do so we will consider a typical formula discussed in Refs. 13 and 14. There, the growth rate γ is reduced from $\sqrt{gk}$ to

$$\gamma = [(kv_A/2)^2 + gk]^{1/2} - kv_A/2 , \qquad (42)$$

where v_A is the ablation velocity. We will extend this to spherical geometry by replacing the integrand in Eq. (26) with Eq. (42). We will include the f_1 factor from Eq. (26), and we will consider a range of values for v_A. Equation (26) is then numerically integrated for each l to give growth factors as plotted in Fig. 5. These growth factors determine the perturbation amplitude at the ablation front after acceleration inward at g_1 for t_1. The initial perturbation values can be multiplied by these growth factors, saturation modeling can be applied, and the squared modes can be summed to determine the bubble amplitude at the ablation front at peak velocity. The resultant amplitudes are shown in Fig. 6. Clearly the ab-
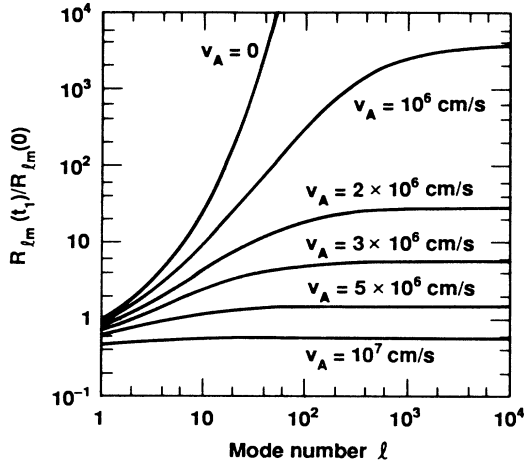
FIG. 5. Linear growth factors at the ablation front for the implosion described in the text. Growth is given by Eq. (42), modified for spherical geometry. Various possible ablation velocities v_A are as indicated.

lation velocity is much more important than the initial value of the perturbation.

If the bubble amplitude as calculated here is greater than the shell thickness at peak velocity, which we have assumed to be 5 μm, then the shell is destroyed by the bubble penetration. This is the case for most initial amplitudes for $v_A < 10^6$ cm/s. However, a sufficiently large v_A will prevent bubble penetration.

It should be emphasized that we are not claiming to have established that ablation velocities greater than 10^6 cm/s will stabilize an implosion. That would require validating Eq. (42), as well as more specific attention to an actual acceleration history. Our purpose is merely to
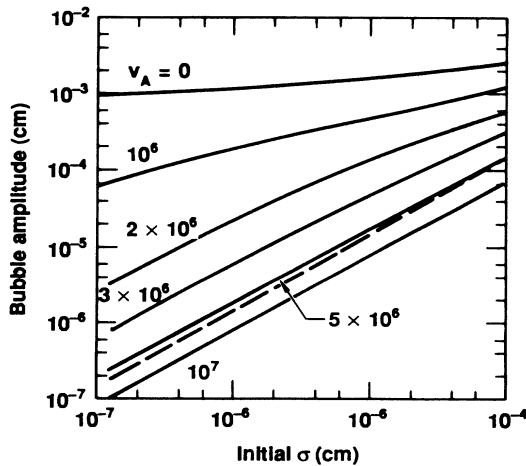
FIG. 6. Calculated net bubble amplitude at the ablation front at peak velocity using growth factors from Fig. 5 for different ablation velocities. The dotted line is $\sigma\sqrt{2}$, representing no amplitude change.

illustrate that, given a description of the single-mode stabilization, one can use this model to estimate the multimode bubble penetration.

Similarly, we can estimate the interface coupling and deceleration phase growth. Recall that the unperturbed shell thickness at peak velocity was assumed to be $T_0 = 5.0$ μm. The perturbed shell thickness is estimated as

$$T_b = \max(0, T_0 - B) \ , \tag{43}$$

where B is the bubble amplitude from Fig. 6. Assume that each mode couples classically through this thinned shell. Then, an amplitude $R_{lm}^{\text{outer}}(t_1)$, on the outside of the shell at peak velocity, produces, on the inside of the shell, an amplitude

$$R_{lm}^{\text{outer}}(t_1)e^{-T_b l/R(t_1)} \ ,$$

where $R(t_1)$ is the average of the inner and outer radii at t_1. In addition to this coupling from the ablation front instability, perturbations on the inside can also be seeded by the initial amplitude on the inside surface itself. This is important for short wavelengths that are stabilized on the outside or do not couple through the shell. Assume for our illustrative purpose that, up until peak velocity, there has been negligible growth (or shrinkage) of these modes from their initial values $R_{lm}^{\text{inner}}(0)$. Since perturbations originally on the inside and outside will have random phase, the typical combined amplitude at peak velocity on the inside will be the quadrature sum

$$|R_{lm}^{\text{inner}}(t_1)| = [R_{lm}^{\text{inner}}(0)^2 + R_{lm}^{\text{outer}}(t_1)^2 e^{-2T_b l/R(t_1)}]^{1/2} \ . \tag{44}$$

These amplitudes now grow in time according to the above deceleration analysis. We can use Eqs. (30) and (31), except that the factor in large parentheses in Eq. (30), representing the initial amplitude, must be replaced with the numerical amplitudes $R_{lm}^{\text{inner}}(t_1)$ calculated above.

Now these final amplitudes on the inside can be summed numerically to give the spike penetration shown in Fig. 7. The lower envelope of those curves shows the effect of the perturbations seeded by initial values on the inside alone. Recall that the imploded radius was 10 μm, so that the predicted spike amplitude is typically a fairly large fraction of this radius unless the ablation velocity is too small. Of course, the predicted spike amplitude depends on the parameters and the other assumptions that describe the target implosion.

E. Extension of the model to two-dimensional perturbations

The model as defined so far has been appropriate for three-dimensional (3D) perturbations on a sphere or plane. Most numerical simulations are run in two dimensions (2D), i.e., they are azimuthally symmetric about some axis in spherical geometry or, in planar geometry, are translationally symmetric in the direction perpendicular to the wave vectors of the perturbations. In order to
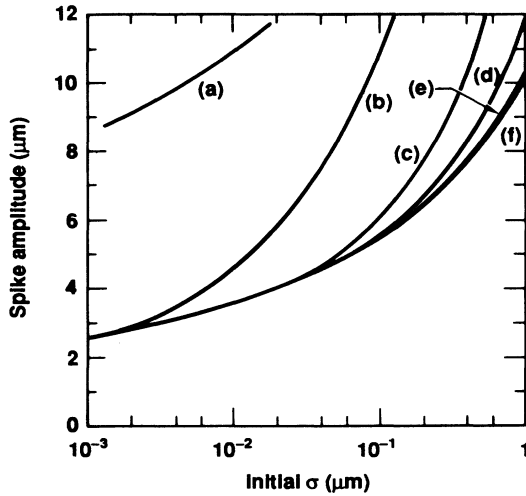
FIG. 7. Calculated penetration of spikes into imploded gas at minimum radius of 10 μm. Curves $(a)-(f)$ represent the same six values of v_A indicated in Figs. 5 and 6. For the larger values of v_A, the curves have converged to a limit representing the perturbation resulting only from the inner surface finish, with no contribution from growth at the ablation front. At very small initial amplitudes these approach $(1+\alpha)(0.07\alpha gt^2)=2.1$ μm.

compare with these calculations, it is necessary to consider how the model is modified for such a situation.

It is straightforward to modify the arguments used above. Once again, it is easier to visualize the physics using planar geometry and Fourier modes. Let $\eta_2\lambda$ be the amplitude at which a single mode saturates. For a full spectrum of modes, we assume that saturation begins for mode k when the rms sum of all modes k' with $|k\pm k'| < k\epsilon$ become equal to $\eta_2\lambda$. Let $S_2(k)$ denote the amplitude at which this occurs. Then we have

$$\eta_2\lambda = \left[4\epsilon k\frac{L}{2\pi}S_2(k)^2\right]^{1/2} , \qquad (45)$$

where, just as in Eq. (14), we have made explicit the three factors of the area over which we are summing, the density of states, and the summand. Equation (45) implies that S_2 is given by

$$S_2(k)=\eta_2[2\pi^3/(\epsilon Lk^3)]^{1/2} . \qquad (46)$$

The dimensionless multiplier $\eta_2(2\pi^3/\epsilon)^{1/2}$ is different from the analogous quantity in 3D, i.e., the quantity ν which is proportional to $\eta\epsilon^{-1}$ according to Eq. (17). In three dimensions $\eta\epsilon^{-1}$ was normalized directly, without independently evaluating η and ϵ. To extend the model to 2D we need to determine them separately. Since our saturation model ties exponential growth immediately to linear growth, η and η_2 are set by the bubble velocity (so that saturation occurs at the level at which the velocity of the growing exponential is equal to the desired asymptotic bubble velocity). Using the bubble-velocity values derived by Layzer[9] and discussed in Ref. 6, we get $\eta_2=0.23/\sqrt{2\pi}=0.092$ and $\eta_3=0.36/\sqrt{2\pi}=0.14$.

Given η_3 and ν we determine that $\epsilon=0.4$. Now we use Eq. (46) in 2D, assuming that we can use the same value of ϵ.

The two scaling rules considered in Sec. III also have their 2D analogues, and the form given by Eq. (46) satisfies them uniquely just as we found in 3D. To calculate the bubble growth with constant acceleration, we could probably do an analytical development parallel to that above. But for our present purposes it is just as useful to do one case numerically. Figure 8 shows the bubble amplitude versus gt^2 in 2D. Note that the initial amplitude in 2D must be considerably larger than that in 3D in order to produce the bubble growth of $0.04\alpha gt^2$ to $0.06\alpha gt^2$ described in Refs. 5 and 6. In 3D the model clearly indicates that $0.07\alpha gt^2$ is close to the lower limit of the bubble amplitudes one can expect to observe (see Fig. 2, where the smallest credible initial amplitudes lead to approximately $0.07\alpha gt^2$). In 2D, this lower limit amplitude from the model is closer to $0.025\alpha gt^2$ than to $0.04\alpha gt^2$, as is evident in Fig. 8.

It appears that the model gives growth in 2D slightly smaller than our current understanding of what it should be. That is unfortunate, because it would be easier to compare the model with 2D code calculations than with 3D experiments. There are several possible explanations for why the model predicts too little net growth in 2D. The argument represented by Eq. (45), using the 3D value of ϵ, could be too simple an estimate. Even in 3D, the details of determining whether a band of modes is reaching net amplitude $\eta_3\lambda$ must be considerably more complicated than we have assumed. For example, we have assumed that whether or not modes affect each other's saturation is determined only by $|k-k'|$, but it seems quite plausible that modes with k and k' parallel, as in 2D, would maintain constructive interference differently than modes with $k-k'$ perpendicular to k. If we conclude
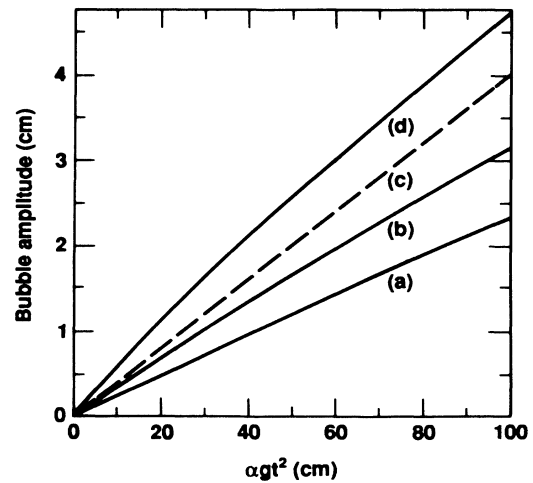
FIG. 8. Calculated bubble growth in two dimensions. The initial spectrum for (a) assumes that $L\langle|Z_k|^2\rangle$ in 2D is equal to $L^2\langle|Z_k|^2\rangle$ in the 3D thermal spectrum used in Figs. 1 and 2. The initial spectra for (b) and (d) are 100 and 10^4 times thermal. Curve (c) is $0.04\alpha gt^2$.

that there must be a new parameter ϵ_2 that represents interference of strictly parallel modes, as in 2D, we could of course normalize the model independently to 2D growth. Finally, it is also possible that the bubble-coalescence phenomenon that is not included in our model is more important in 2D.

VI. CONCLUDING DISCUSSION

There is a fairly widely held opinion that late-time Rayleigh-Taylor growth is nearly independent of initial amplitude, with long-wavelength modes being seeded by nonlinear interactions from the short-wavelength modes. That may indeed be the case, but the results presented here suggest that we must be careful about how strong the case for this scenario has been made. Our simple model, which does not include any bubble coalescence or other nonlinear mode coupling, nevertheless gives very reasonable looking results for a wide variety of situations. Perhaps nonlinear mode coupling is not as important as many have come to believe.

Long-wavelength modes can be seeded in various ways. Of course, they can be seeded by the actual initial perturbation, as we have considered here. They can also be seeded by nonlinear coupling from short-wavelength modes in the manner generally thought to be important. The question opened up by this work is the relative importance of these two seeds. Clearly, in a situation where the initial amplitudes of all long-wavelength modes are orders of magnitude less than the initial amplitudes of short wavelength modes, the nonlinear coupling is the only seed for these modes and must dominate. However, in most physical situations the initial spectrum is a decreasing function of k (or l), and it is not obvious that the seeding by nonlinear effects dominates the growth that arises from what perturbation was there initially.

It would be convenient if growing multimode perturbations were in fact independent of initial amplitude, since we could then attempt to calculate final perturbations without detailed knowledge of the initial spectrum. Such a situation could also relax considerably the requirements of target fabrication technology. Unfortunately, it is not clear that nature has been so kind. The criterion that the initial amplitude matters if it is larger than about 0.01λ appears to be correct for a single mode. However, the criterion should be phrased more precisely: i.e., one calculates the growth of the single mode, including saturation, and compares that amplitude to $0.07agt^2$. It is very unlikely, however, that this criterion can be sensibly applied to a broadband initial spectrum of long-wavelength modes.

It should be noted that, although the model appears to give sensible results for the net perturbation amplitude, we have not checked whether the calculated spectrum is at all in accord with experiment or with simulation. It is possible that the actual spectrum is more heavily dominated by the longer wavelengths, these having been seeded in their growth by the prior growth of the shorter wavelengths. It may be that our model takes into account the contribution of the short wavelengths, which in reality could contribute by seeding the growth of long wavelengths, by letting them grow somewhat more than they should. (Note that we have neglected at least one physical effect that could slow the growth of short-wavelength modes: the density gradient introduced by the growing mixed region.) The model has been normalized to give the sum over modes correctly for one situation (constant acceleration and planar geometry). If it is getting the spectrum wrong, our hope is that this approximate way of taking into account the contribution of the short wavelengths can be extended to other situations as well. We conclude with some comments regarding the applicability of the model proposed here.

First, the model cannot be meaningfully applied if the perturbation growth significantly changes the zeroth-order physics. In that case, the notion of calculating the growth of individual modes with linear analysis is clearly wrong. Equation (43) represents one attempt to compensate for such an effect, but such *ad hoc* fixes are of limited generality.

Second, we are assuming that the long-wavelength modes are predominantly seeded by the physical initial amplitudes rather than by nonlinear mode coupling. Of course, it is difficult to ascertain the validity of this in any particular situation (if it is ever valid). But one would expect the model to give incorrect results for situations where the long-wavelength modes have very small initial amplitudes—i.e., decades smaller than the initial amplitudes of a broadband of short-wavelength modes.

The third qualification regarding the applicability of the model is a practical one. We are limited in our ability to calculate the growth of single modes and to determine their initial conditions. Precise calculations are not necessarily needed. In the above examples we saw circumstances where multiple orders of magnitude in initial condition or growth factor only changed the bubble amplitude slightly. Nevertheless, there may be circumstances where one is unable to obtain sufficiently accurate single-mode characteristics.

In general, the model appears to be most useful for making estimates of multimode perturbation growth in circumstances in which (i) there is not too much growth, so that the model is only a small extension of linear analysis and (ii) the growth which does occur is dominated by low l modes, because these are easier to simulate with existing codes. Thus the model is especially well suited for projecting performance of high gain future ICF capsules, in which ablative stabilization plays a more important role than in many current targets. This application alone is of considerable importance.

[1]Lord Rayleigh, *Scientific Papers* (Cambridge, University Press, Cambridge, England, 1900), Vol. II, p. 200.

[2]G. I. Taylor, Proc. R. Soc. London, Ser. A **201**, 192 (1950).

[3]D. H. Sharp, Physica **12D**, 3 (1984).

[4]M. J. de C. Henshaw, G. J. Pert, and D. L. Youngs, Plasma Phys. Controlled Fusion **29**, 405 (1987).

[5]D. L. Youngs, Physica **12D**, 32 (1984).

[6]K. I. Read and D. L. Youngs, Atomic Weapons Research Establishment Report No. 011/83, Aldermasten, 1983 (unpublished).

[7]W. P. Crowley, Lawrence Livermore Laboratory Report No. UCRL-72650, 1970 (unpublished).

[8]In unpublished notes, D. L. Youngs makes an argument somewhat similar to this in order to estimate the duration of linear growth for fluids with viscosity, given a broadband initial spectrum of modes on a Rayleigh-Taylor unstable interface.

In that case, the spectrum is dominated by a narrow band around a fastest-growing mode k_m, with the width of the band determined by the growth rate at $k \ll k_m$ and by the viscosity at $k > k_m$. To my knowledge he has not suggested, as I do here, that saturation can be determined, in general, by summing over a bandwidth proportional to k.

[9]D. Layzer, Astrophys. J. **122**, 1 (1955).

[10]J. Lachaise, A. Graciaa, A. Martinez, and A. Rousset, Thin Solid Films **82**, 55 (1981).

[11]F. Hattori, H. Takabe, and K. Mima, Phys. Fluids **29**, 1719 (1986).

[12]I. S. Gradshteyn and I. W. Ryzhik, *Table of Integrals, Series, and Products* (Academic, New York, 1965).

[13]S. E. Bodner, Phys. Rev. Lett. **33**, 761 (1974).

[14]M. H. Emery, J. H. Gardner, and S. E. Bodner, Phys. Rev. Lett. **57**, 703 (1986).